Characterization of Double-Strand Break Repair Protein Ku80 Location Within the Murine Retina

Brigitte Müller, Franziska Serafin, Leonie Luise Laucke, Wilhelm Rheinhard, Tobias Wimmer, and Knut Stieger

Department of Ophthalmology, Justus-Liebig-University Giessen, Giessen, Germany

Correspondence: Brigitte Müller, Department of Ophthalmology, Faculty of Medicine, Justus-Liebig-University Giessen, Aulweg 123, 35392 Giessen, Germany; brigitte.mueller@augen.med.uni-giessen.de.

Received: July 30, 2021
Accepted: May 14, 2022
Published: June 23, 2022

Citation: Müller B, Serafin F, Laucke LL, Rheinhard W, Wimmer T, Stieger K. Characterization of double-strand break repair protein Ku80 location within the murine retina. *Invest Ophthalmol Vis Sci.* 2022;63(6):22. https://doi.org/10.1167/iovs.63.6.22

Purpose. To characterize the spatial distribution of the DNA-double strand break-repair protein Ku80 in the murine retina. Even though robust data exist on the complexity of DNA repair mechanisms in dividing cells in vitro, almost nothing is known about it in post-mitotic neurons or photoreceptors (PRs). This knowledge is an important prerequisite for in vivo therapeutic approaches by genome editing in retina and PRs. Recently, it was shown that mouse rod PRs are incapable of repairing double-strand breaks induced by radiation.

Material and Methods. Retinae from wild-type, rd10, and RPGR-KI mouse lines were obtained and stained with antibodies against Ku80, and cellular markers CtBP2, beta-Dystropglycan, Lamin B, and peanut agglutinin. Organotypic explant cultures were generated and maintained for up to 10 days. Laser microdissection was performed to obtain photoreceptor nuclei, and Ku80 expression was compared to whole retina by real-time PCR (RT-PCR).

Results. Strong Ku80 immunoreactivity was observed in rod but not cone photoreceptor terminals localized in the outer plexiform layer of the retina in all three mouse lines. During retinal explant culture, we observed that Ku80-positive globules translocate into the heterochromatin region of nuclei in the outer nuclear layer (ONL). By quantitative PCR, we showed upregulation of relative *Ku80* expression in the ONL during wild-type retinal explant culture.

Discussion. The unexpected localization of Ku80 to murine rod terminals indicates another tissue-specific modification to the canonical DNA repair mechanisms and warrants further investigation.

Keywords: DNA repair, photoreceptor cells, retinal explant, mouse retina, gene editing

In the retina, several hundred proteins are uniquely expressed, and mutations in more than 200 genes have been associated with inherited retinal diseases.[1,2] Therapeutic genome editing represents a promising emerging field in the treatment of monogenic disorders.[3] Genome editing is based on the cells' own capacity to repair DNA double-strand breaks (DSB). The idea of using this physiological mechanism to repair disease-causing mutations is comparatively young and relies on highly specific endonucleases and the capacity of the cell to repair DSBs.[4,5] After the introduction of a DSB by highly specific endonucleases, the cell's own DNA repair machinery restores integrity to the DNA strand. This happens either through the error-prone non-homologous end-joining (NHEJ) pathway or with high fidelity through homology-directed repair (HDR) in the presence of a DNA donor template.[5] An alternative repair pathway called micro homology-mediated end joining (MMEJ) has also been discovered.[6]

Even though robust data exist on the complexity of DNA repair mechanisms in dividing cells in vitro, almost nothing is known about it in postmitotic neurons or photoreceptors (PRs). The current understanding is that NHEJ represents the predominant pathway at all cell-cycle stages in mitotic cells, whereas HDR (G2) and MMEJ (G1) are only active during certain phases of the cell cycle.[7] However, the situation seems to be different in PRs: it has recently been shown that mouse rod PRs are incapable of repairing DSBs induced by radiation as measured by quantification of repair foci over time.[8] This deficit might be associated with changes to the nuclear architecture, as mouse rod PRs exhibit an inverted version of chromatin associated with a lack of lamin B and lamin B receptor expression.[9] However, recent results indicate that after ionizing radiation, the DSB repair efficiency in rods correlates with the level of Kruppel-associated protein-1 expression and its ataxia-telangiectasia mutated–dependent phosphorylation and therefore does not result from their specialized chromatin organization.[10]

In vitro studies have indicated that HDR or MMEJ activity can be increased by blocking the NHEJ pathway, a strategy that could potentially help in performing high-fidelity DNA repair in the retina in vivo.[11,12] Within the immensely complex DNA repair machinery, few proteins have gathered particular attention because of their important position at decision-making steps in the cascade of protein-protein

interactions. Previous studies by our group indicated that in contrast to what has been observed in cell culture studies, presence of yH2AX at DSB sites does not result in the recruitment of 53bp1,[13] which indicates potentially alternative mechanisms involved in DNA repair. Observations like this highlight the necessity to study DNA repair proteins in photoreceptors and the retina in more detail.

Based on the existing knowledge generated in cell culture studies, Ku80, encoded by the X-ray repair cross-complementing protein 5 gene (*XRCC5*) in humans, is involved in the first step of the NHEJ pathway by recognizing the DSB together with the Ku70 (*XRCC6*) protein. Both proteins together form a heterodimer called Ku. The heterodimer protects the DSB against nucleolytic degradation by binding the ends of broken DNA double strands tightly with high affinity, has catalytic activity and recruits other core NHEJ factors, like DNA-PKcs.[14–17] Additionally, the Ku80 protein comprises 5′-dRP/AP lyase activity that excises abasic sites (AP) near double-strand break ends.[16,17]

Ku80 is also involved in multiple cellular processes like the cell cycle control, transcription, telomere maintenance, proliferation, and apoptosis.[18–20] Although the regulation of all diverse functions of Ku is unclarified as yet, it has been shown that the control mechanisms underlying the heterodimerization and subcellular localization of Ku70 and Ku80 play, at least in part, a key role in regulating the physiological function of the Ku heterodimer.[21,22] Ku80-knockout mice exhibit not only deficiencies in DSB repair, but also growth retardation.[23,24]

In the present study, we examined the expression and localization of Ku80 in both PR types and in other neurons in the murine retina of wild-type, rd10, and RPGR-KI mice, and in organotypic retina cultures as a well-defined degeneration model. We observed an unexpected localization to the rod spherules, but not cone pedicles in all model systems tested and lower levels in the inner retina. Upon degeneration, Ku80 staining changes its localization to the outer nuclear layer. We subsequently introduced laser microdissection to study gene expression in PR cells and compared the data to the inner retina. We observed a significant increase in Ku80 expression levels in the photoreceptor layer as compared to the inner retina.

Materials and Methods

Experimental Design

Fifty adult animals per mouse line between three and nine months of age as well as four immature wild-type mice were included in this study comprising both sexes. At least three eyes from different individual mice were used for histologic analysis and at least three eyes from different individual mice were used for quantitative PCR (qPCR) analysis (whole retina or laser capture microdissection [LCM]) of each explant culture period. Young rd10 and C57BL/6J were investigated at p30. At least two immunostaining procedures were performed for each antibody and each investigated mouse tissue of the respective mouse lines and ages. For microscopic analysis, two or three sections of each immunostaining per respective mouse line and age were analyzed.

Ethics Statement

All procedures concerning animal handling and euthanizing complied with the European legislation of Health Principles of Laboratory Animal Care in accordance with the ARVO Statement for the Use of Animals in Ophthalmic and Vision Research and were proofed by the German animal welfare act (TV-No M_474).

Mouse Models and Animal Handling

Wild-type C57BL/6 mice (Jackson stock no. 000664; Charles River, Sulzfeld, Germany) and RPGR-KI mice (B6J.SV129-*Rpgr*^{tm1stie}) were used in this study. We have generated the mouse model RPGR-KI for X-linked retinitis pigmentosa (XLRP) due to mutations in the retinitis pigmentosa GTPase regulator (*RPGR)* gene. The mouse develops a mild phenotype with significant loss of photoreceptors starting at nine months of age.[25] Mice were housed and bred in the animal facility of the University of Giessen under a cycle of 14-hour light (200 lux illumination in the cage) and 10-hour dark. Immature rd10mice (RRID:MGI:3581193) and their respective wild-type strains C3H and C57BL/6J were subjects in this study and were provided by François Paquet-Durand from Tübingen. Retinal degeneration 10 (rd10) mice carry a spontaneous mutation of the rod-phosphodiesterase gene, leading to a rod degeneration that starts around P18.[26]

Preparation of Organotypic Retina Culture

Organotypic retina culture was performed as described previously.[13,27] In brief, explanted retinas were cultured on track-etched polycarbonate membrane, pore size 0.4 µm and 30 mm in diameter (no. 35006; Laboglob.com GmbH, Gottmadingen, Germany), with the photoreceptor layer facing the supporting membrane. Inserts were put into six-well culture plates and incubated in complete medium with supplements at 37°C. Complete culture medium was a composite made of 50% Dulbecco's modified Eagle medium (PAN Biotech, Aidenbach, Germany), 25% fetal bovine serum (PAN Biotech), and 25% HBSS supplemented with 2 mM L-glutamine (PAN Biotech), 5.75 mg/mL glucose, and antibiotics (100 µg/mL streptomycin and 100 units/mL penicillin; PAN Biotech). Every second day the full volume of complete medium, 1.2 ml per well, was replaced with fresh medium. The culture period was ended by immediate fixation in 4% paraformaldehyde in phosphate buffered saline solution (PBS) for 45 minutes at time points ranging from two to 10 days. Fresh (i.e., un-cultured) retinas were used as controls.

$KBrO_3$ Incubation Procedure (Positive Control for Ku80 WB and Immunohistochemistry)

To initiate DNA DSBs, adult RPGR-KI mouse retina was dissected in Hanks' balanced saline solution (GIBCO HBSS; no. 14025076; Thermo Fisher Scientific, Waltham, MA, USA) or PBS, transferred into a 2 mL Eppi and incubated in 0.15 mM or 1.5 mM $KBrO_3$ (no. 4396; Roth, Germany) for 1.5 hours at 37°C. Working solution of $KBrO_3$ was prepared with pure water.[13] Subsequently, all treated retinal tissues were briefly rinsed in HBSS or PBS and either immediately frozen in liquid nitrogen for lysis of WB analysis or fixed in 4% paraformaldehyde in PBS at room temperature for 45 minutes. After washing in PBS, all treated retinal tissue was cryo-protected in graded sucrose solutions (10%, 20%, and 30% in PBS), frozen, cut, and immunostained with Ku80 antibody (see next section).

Investigative Ophthalmology & Visual Science

Table 1. Primary Antibodies

Antigen	Description of Immunogen	Source, Host Species, Cat. No., Clone or Lot No.	Concentration Used
Ku80	Synthetic peptide corresponding to the carboxy terminus of human Ku80.	Cell Signaling, rabbit, polyclonal antibody, Cat. no. 2753	ISH 1:300; WB 1:1,000
Ku80 blocking peptide		Cell Signaling, Blocking Peptide for AB 2753, Cat. no. 92918	1:150 (1 mg/mL)
CtBP2	Mouse CtBP2 aa. 361-445	BD Transduction Laboratories, mouse monoclonal antibody, Cat. no. 612044, Clone 16/CtBP2	1:5,000
β-Dystroglycan	Synthetic peptide containing 15 of the last 16 carboxyl-terminal amino acids of human β-dystroglycan. PKNMTPYRSPPPYVP-PCOOH	Leica Biosystems Newcastle Ltd, UK; Novocastra Lyophilized mouse monoclonal antibody Beta-Dystroglycan, Cat. no. NCL-b-DG, clone 43DAG1/8D5	1:200
PNA	Lectin PNA From Arachis hypogea (peanut), Alexa Fluor 488 Conjugate is specific for terminal β-galactose	Thermo Fisher Scientific, Cat. no. L-21409	1:300
LaminB_2	66 kD lamin B2 isoform of LaminB_2	Thermo Fisher Scientific, mouse monoclonal, Cat. no. 33-2100, Clone: E-3 RRID: AB_2533107	1:200
GAPDH	Synthetic peptide near the carboxy terminus of human GAPDH.	Cell Signaling, GAPDH (14C10) Rabbit monoclonal antibody, Cat. no. 2118	WB 1:10,000

Tissue Processing and Immunohistochemistry

For frozen sectioning, immature and adult mouse eyecups and retinal explants were treated as described previously.[27] Immunostaining was performed employing the two-step indirect method. Prior to Ku80 antibody staining, antigen retrieval was performed.[28] Sections were incubated at room temperature overnight in primary antibodies (see Table 1). Immunofluorescence was performed using Alexa Fluor 488-conjugated secondary antibodies (no. 21202; Thermo Fisher Scientific) or Alexa 594 (no. 21207; Thermo Fisher Scientific). Vertical frozen sections of nine-month-old C57BL/6J mice harvested after two days of retinal explant culture were used to validate polyclonal Ku80 antibody with a Ku80 blocking peptide (Figs. 1B, 1C). A cocktail containing two parts of the blocking peptide Ku80 (1 mg/mL) and one part of the polyclonal Ku80 antibody (35 µg/mL) was preincubated for 30 minutes before incubation on the retinal sections.

Laser Scanning Confocal Microscopy

Confocal images were taken using an Olympus FV10i confocal microscope, equipped with Argon and HeNe lasers. High-resolution scanning of image stacks was performed with a UPlanSApo x60/1.35 (Olympus, Tokyo, Japan) oil immersion objective at 1024 × 1024 pixels and a z-axis increment of 0.3 µm. For analysis of immunolabeled cells and their processes, a stack of two to 12 sections was taken (0.7-µm z-axis step size). Cell processes were reconstructed by collapsing the stacks into a single plane. Brightness and contrast of the final images were adjusted using Adobe Photoshop CS5 (San Jose, CA, USA).

Laser Capture Microdissection

Eyes were enucleated, cultivated for a defined period (up to eight days) or embedded directly in TissueTek without fixation and snap-frozen in liquid nitrogen. Tissues were stored at −80°C until LCM. Eight-micrometer–thick sections were cut at −20°C and mounted on PEN-Membrane slides (no. 11505158; Leica, Wetzlar, Germany). Before LCM, morphology was exposed. Therefore sections were stained with hematoxylin for 40 seconds, washed with water (2 × 2 seconds), and dehydrated with ethanol: 2 × 70% ethanol, 2 × 96% ethanol, 3 × 100% ethanol, each for two seconds. Slides were removed from ethanol and air-dried. The system LSM 6000 (Leica) was used for LCM. For collecting the outer nuclear layer and inner retina separately, small tubes (no. 04.100.0100; Nerbe Plus, Winsen, Germany) filled with 30 µL RLT Buffer (from QIAGEN RNeasy Micro Kit; Qiagen, Hilden, Germany) containing 0.001% β-mercaptoethanol were used. Approximately 40 sections were collected per retina and retinal layer. Immediately after LCM, the samples were vortexed for 15 seconds, snap-frozen in liquid nitrogen, and stored at −80°C until RNA isolation. RNA isolation was performed as described below. The quality and quantity of the RNA were assessed with NanoDrop 2000 (Peqlab, Erlangen, Germany).

Gene Expression Analysis by qPCR

Three fresh retinas or retinal explants were pooled and homogenized with a Precellys homogenizer (Peqlab, Erlangen, Germany) using Precellys CK14S vials for 25 seconds at 2800 g. Also, other tissues and cells were homogenized with the Precellys homogenizer. Total RNA was purified via RNeasy Micro Kit (no. 74004; Qiagen) or RNeasy Mini Kit (no. 74104; Qiagen) depending on sample size and according to protocol. The cDNA was synthesized with PrimeScript RT Master Mix (no. RR036Q; Takara, Saint-Germain-en-Laye, France). Sequences of primers are listed in Table 2. The real-time qPCR system Mastercycler ep realplex (Eppendorf, Hamburg, Germany) was used. To reduce confounding variance, three independent biological samples from different littermates were analyzed in technical triplicates, which were averaged before fold change calculation. The delta delta Ct method ($\Delta\Delta$Ct) was used to analyze the relative mRNA levels.[29] Uncultured retinas (0 days in culture) served as the control group. For qPCR analysis of the whole retina, glyceraldehyde-3-phosphate-dehydrogenase (Gapdh)

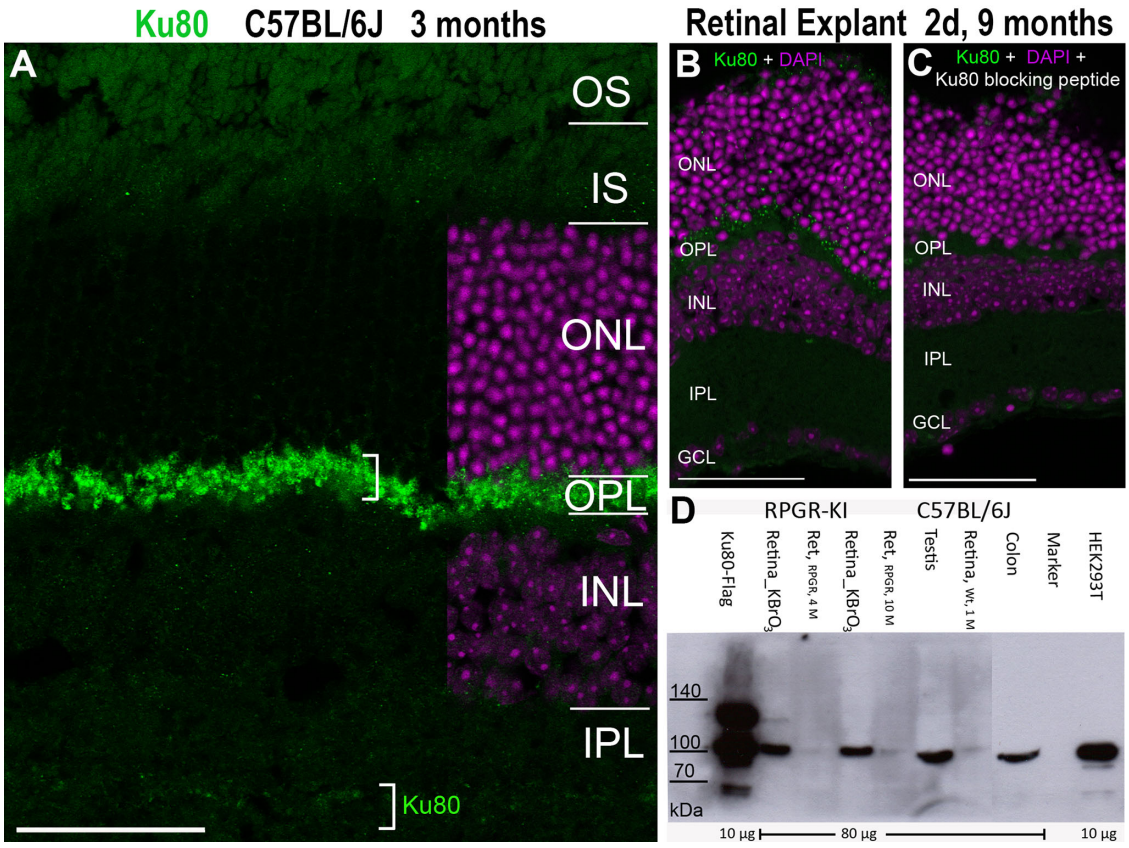

Figure 1. Validation of the Ku80 antibody. (**A**) Vertical frozen section of three-month-old C57BL/6J mouse. Strong Ku80 immunoreactivity (*green*) is obvious throughout the OPL and in a weak spotty manner also in the IPL, the level marked by the *bracket*. For magnification reasons the inner part of the IPL and the GCL are not shown. (**B, C**) Validation of polyclonal Ku80 antibody with Ku80 blocking peptide in retinal explants of nine-month-old C57BL/6J mice after two days in culture. (**B**) Numerous Ku80-ir beadlets (*green*) are obvious in the OPL and some in the ONL also. (**C**) No Ku80-ir staining at all in the OPL and ONL after staining with a cocktail of Ku80 blocking peptide and Ku80 antibody preincubated for 30 minutes. Single immune labeling (*green*) is displayed in combination with DAPI staining (*magenta*). (**D**) In Western blot analysis of Ku80 protein lysate of untreated HEK293 cells, as well as treated HEK293 cells transfected with eGFP-FLAG-Ku80, served as positive controls. Radioimmunoprecipitation assay buffer was used to prepare the tissue and cell lysates: 80 µg and 10 µg protein were loaded, respectively. The HEK293 cells transfected with eGFP-FLAG-Ku80 plasmid showed three Ku80 immunoreactive bands altogether (**D,** *lane 1*). The middle band at 100 kD corresponds with the Ku80 band of untreated HEK293 cells, different to the mouse retina samples, and the testis and colon tissue. The higher band at 120 kDa corresponds to the FLAG tagged Ku80 protein. Treatment of RPGR-KI whole retina for 1.5 hours with 1.5 mM or 0.15 mM $KBrO_3$ revealed increased amount of Ku80 protein (*lanes 2* and *4*). Almost no difference in Ku80 protein amount is visible between the two $KBrO_3$ concentrations. In untreated RPGR-KI retina a very faint Ku80 band is visible (*lanes 3* and *5*). Similarly low Ku80 protein amount is visible in untreated wild-type retina (*lane 7*). In wild-type tissue of testis and colon, the amount of Ku80 protein looks similar to the $KBrO_3$ treated RPGR-KI retina. IS, inner segments; GCL, ganglion cell layer. *Scale bars* in A,B,C: 50 µm.

Table 2. Primer Sequences

Primer Name	Primer Sequence	Amplicon Size
Murine 18 S rRNA forward	5′-GACACGGACAGGATTGACAGATT-3′	206 bp
Murine 18 S rRNA reverse	5′-TCAATCTCGGGTGGCTGAA-3′	206 bp
Murine Gapdh forward	5′-GGTCGGTGTGAACGGATTTGG-3′	208 bp
Murine Gapdh reverse	5′-CCCGTTGATGACAAGCTTCCC-3′	208 bp
Murine Ku80 forward	5′-GCAGCAAAGGATGATGAGGC-3′	156 bp
Murine Ku80 reverse	5′-CTCATAGGCGTCCTTAATGTAAGG-3′	156 bp

was applied as the housekeeping gene (reference gene), for analysis of LCM material *18SrRNA* was used for this purpose. All samples collected with the LCM method were checked with rhodopsin as a marker gene for the ONL to detect potential cross-contamination between individual retinal layers. Subsequently, real-time qPCR for *Ku80* was performed. The Delta-Ct-values were normalized to uncultured retina (day 0, Delta-Delta-Ct-values) (i.e., relative *Ku80* gene expression of uncultured retina represents the value 1).

Western Blot

Neuroretinas (n = 3) from one- and three-month-old wild-type animals C57BL/6J, as well as one-, four-, and

10-month-old RPGR-KI animals, were harvested and lysed using the radioimmunoprecipitation assay buffer. Lysate of HEK293 cells transfected with the pEGF-C1-FLAG-Ku80 plasmid (no. 46958; Addgene Europe, Teddington, UK) and native HEK293 cells served as positive controls. Eighty and 100 µg of total protein extract was analysed by SDS-PAGE (10%) and immunoblotting using the Ku80 antibody, which identifies an epitope in the carboxy terminus of human Ku80 (Table 1).

Statistical Analysis

Statistical comparisons among different experimental groups were made using a two-tailed Student's *t*-test and SigmaPlot 12 software. Error bars indicate standard deviation (SD).

Results

Unexpected Immunohistochemical Localization of Ku80 in the Outer Plexiform Layer

In three-month-old wild-type mouse retina, we observed a defined line of Ku80 positive staining in the outer plexiform layer and to a lesser extent in the inner plexiform layer (Fig. 1A). Specificity of the antibody was verified by incubating the slides with Ku80 blocking peptide (Figs. 1B, 1C), as well as by Western blot analysis of whole retina protein, which revealed a band at the expected size of about 100 kDa (Fig. 1D).

Treatment of RPGR-KI whole retina for 1.5 h with 1.5 mM or 0.15 mM $KBrO_3$ revealed increased amount of Ku80 protein (Fig. 1D, lanes 2 & 4). Almost no difference in Ku80 protein amount is visible between the two $KBrO_3$ concentrations. In untreated RPGR-KI retina only a very faint Ku80 band is visible (Fig. 1D, lanes 3 & 5). Similarly low Ku80 protein amount is visible in untreated wild-type retina (Fig. 1D, lane 7). In wild-type tissue of testis and colon, the amount of Ku80 protein looks similar to the $KBrO_3$-treated RPGR-KI retina. In the positive control, the human HEK293 cell line a single Ku80 protein band was at about 100 kDa. The HEK293 cells transfected with eGFP-FLAG-Ku80 plasmid showed three Ku80 immunoreactive bands altogether (Fig. 1D, lane 1). The middle band at 100 kDa corresponds with the Ku80 band of untreated HEK293 cells, different from the mouse retina samples, and the testis and colon tissue. The higher band at 120 kDa corresponds to the FLAG tagged Ku80 protein. The lower band at 60 kDa might be a truncated Ku80 protein. Different composition of the Ku80 protein because of post-translational modifications could be the cause for the slightly different migration of Ku80 protein bands.

To verify Ku80 localization early in healthy as well as degenerate retina, we examined one-month-old wild-type and rd10 mouse retina in more detail and tried to identify the cellular compartment of its storage (Fig. 2). We double immunolabeled mouse frozen sections with Ku80 and peanut agglutinin (PNA) (Figs. 1A, 1B). PNA is localized in cone outer segments and synapses, the cone pedicles. This staining clearly revealed that Ku80 did not colocalize with cone pedicles (A', B'). In healthy mouse retina, double immunolabeling with Ku80 and CtBP2, the latter labeling ribbon-like structures in photoreceptor synapses showed a partial colocalization in the outer plexiform layer (OPL) (Figs. 2C, 2D). By colocalization we describe the two proteins Ku80 and CtBP2 being localized in the same anatomical structure, the rod spherule. Both immunolabeled proteins appeared side by side in the rod spherules (Fig. 2C'). Although in rods the CtBP2-ir ribbons showed the typical horseshoe-like shape assigning the layer of the rod spherules within the OPL, the ribbons were lining up in cone pedicles below and outside the Ku80 staining in the OPL (Figs. 2C', 2C″, 2D', 2D″). Similarly, double immunolabeling with Ku80 and β-Dystroglycan revealed that Ku80 was clearly localized in rod spherules but not in cone pedicles (Figs. 1E, 1F). Beta-dystroglycan immunoreactivity was present in the synapses of both photoreceptor types (Fig. 1E', E″, F', F″). It is a central component of the membrane-spanning dystrophin-glycoprotein complex and thought to be important for differentiation of the neuromuscular junction.[30,31] The β-dystroglycan antibody has been extensively used in retinal tissue from different species.[32–35] Immunohistochemical analysis of Ku80 in the retina of one-month-old C57BL/6J mice and rd10 mouse model revealed a similarly unexpected localization yet less obvious due to degeneration of the photoreceptors recognizable by a very thin ONL (Figs. 2B, 2D, 2F).

Because the degeneration the rd10 mouse is quite rapid, we also investigated the localization of Ku80 in the RPGR-Ki mouse, which was recently published by our group and shows a slow progressive degeneration starting at about nine months of age.[25] In adult wild-type and RPGR-KI mice, we observed the same subcellular localization of Ku80 immunolabeling in combination with PNA, CtBP2, or β-Dystroglycan antibodies (Fig. 3).

Release of Ku80 During Retinal Explant Culture

To elucidate functional consequences of the Ku80 storage in rod terminals, we assessed the kinetics of the storage in a standard model for neurodegeneration in the retina, the organotypic retina culture.[27] In such a model, photoreceptors start to degenerate within a few days of culture, and after eight days, more than 50% of nuclei in the outer nuclear layer is gone.[27] Ku80 immunohistochemistry on vertical frozen sections of nine-month-old wild-type and RPGR-KI mice were evaluated after zero, two, four, six, or eight days in culture (Fig. 4). Strong Ku80 immunoreactivity was obvious in the OPL of the retina at day 0 (Figs. 4A, 4F). Between day 2 and 4 of the explant culture, when degenerative processes have started, Ku80 immunoreactive (ir) globules of the OPL begin to be translocated into the ONL (Figs. 4B, 4G, 4C, 4H). After six days in culture, when degenerative processes in the ONL got more pronounced, the release of Ku80 globules into the ONL became a little less (Figs. 4D, 4I). After eight days in culture, the release of Ku80 globules into the ONL was still detectable (Figs. 4E, 4J). In addition, especially in the inner plexiform layer (IPL) of RPGR-KI mice Ku80 immunoreactivity was visible in a week spotty manner (Figs. 4F–H, 4J). Weak nuclear Ku80 immunoreactivity only occurred in nuclei of the inner nuclear layer (INL) in wild-type mice after eight days in culture (E). In RPGR-KI mice only very faint Ku80 immunoreactivity was detectable in INL nuclei after four days in culture (H).

More examples of Ku80-ir globules released into the ONL are shown in wild-type mice, up to 10 days in culture (Figs. 5B, 5C, 5E, 5F). To identify the cellular compartment, to which the Ku80 globules were translocated during explant culture (i.e., neurodegeneration), double immunohistochemical staining of Ku80 and Lamin B, as well as CtBP2 and Ku80, was performed and evaluated. Lamin B

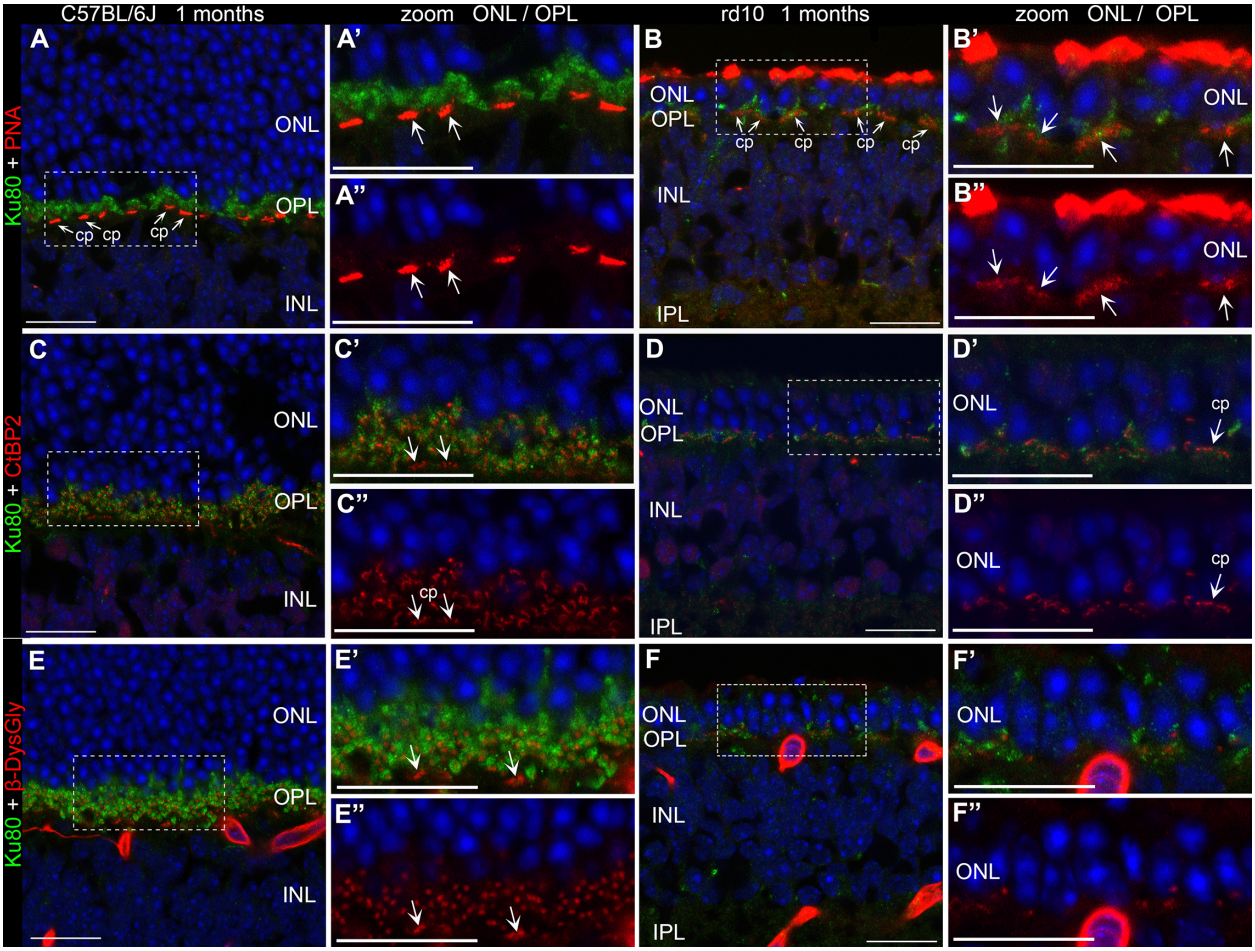

Figure 2. Unexpected localization of Ku80 in rod photoreceptor synapses in the retina of one-month-old C57BL/6J mice and rd10 mouse model. Double and single immunolabeling are displayed in combination with DAPI staining (blue). (**A, B**) Double immunolabeling of Ku80 (*green*) and PNA (*red*). Double immunolabeling of Ku80 (*green*) and CtBP2 (*red*). DAPI counterstaining (*blue*) reveals the retinal nuclear layers. (**A', A'', B', B''**) Magnification of the OPL. PNA is localized in cone photoreceptor outer segments and synapses, the cone pedicles (*arrows*). Ku80 immunostaining does not co-localize with cone pedicles (**A', B'**). (**C, D**) CtBP2 labels ribbon-like structures in photoreceptor synapses. Numerous horseshoe-shaped rod ribbons are visible in the OPL assigning the layer of the rod spherules (**C''**). CtBP2-ir ribbons are lining up in cone pedicles below and outside the Ku80 immunolabeling in the OPL (**C'**) (*arrows*). (**C', C'', D', D''**) Magnification of the OPL. (**E, F**) Double immunolabeling of Ku80 (*green*) and β-dystroglycan (*red*). Beta-dystroglycan is present in all photoreceptor synapses. *Arrows* indicate β-dystroglycan immunolabeling in cone pedicles (**E', E'', F', F''**). The strongly labeled red profiles are cross-sectioned blood vessels (capillaries) detected by the secondary antibody directed against mouse. (**B, D, F**) In one-month-old rd10 mice the ONL is only 2 nuclei thick because of degeneration of photoreceptors. IS, inner segments; cp, cone pedicle. *Scale bars*: 20 µm.

protein is located in the nuclear membrane and helps tethering the DNA there.[36] The Ku80-ir globules were observed close to the Lamin B-ir nuclear membrane in rod PR nuclei (Figs. 5A–C', arrow + asterisk). Additionally, the same sections counterstained with DAPI showed Ku80-ir globules within the lightly stained euchromatin area located in the periphery of the murine rod RP nuclei (Figs. 5A'–C', arrows). Ku80-ir globules in the euchromatin region of rod photoreceptor nuclei could be a sign of DNA DSB repair activity. Double immunolabeling with CtBP2 and Ku80 showed dislocation of ribbon synapses into the ONL in addition to the translocated Ku80-ir globules during retinal explant culture (Figs. 5D–F'). After 10 days in culture, very few CtBP2-ir ribbon synapses are left in the OPL and none in the ONL due loss of photoreceptor cells during retinal explant culture (Figs. 5F, 5F'). Dislocation of rod photoreceptor synapses at early days during retinal explant culture are in line with the degenerative processes starting with separation of the retina from the blood supply and the retinal pigment epithelium.

In one of our previous studies, we used potassium bromate ($KBrO_3$) to induce DSBs in the mouse retina and retinal explants culture of C57BL/6J mice showed colocalization of γH2AX and 53bp1.[13] $KBrO_3$ is an oxidizing agent used as a food additive, which causes kidney damage as a potent nephrotoxic agent, and the mechanism is explained by the generation of oxygen free radicals that induce many DSB and thus cause genomic instability leading to apoptosis.[37] Here we incubated whole RPGR-KI mouse retina (Fig. 6C) in 0.15 mM KBrO3 to initiate DSBs. Control retinae were treated with plain water only (Fig. 6A). In untreated retina, Ku80 is localized in the OPL as shown in Figures 3 and 4. In the ONL no Ku80 immunoreaction could be observed (Fig. 6A). Treated retina revealed Ku80 immunoreactivity in some photoreceptor nuclei in the ONL, possibly cones (Fig. 6C', 6C'', 6D', 6D''). No Ku80 immunoreactivity

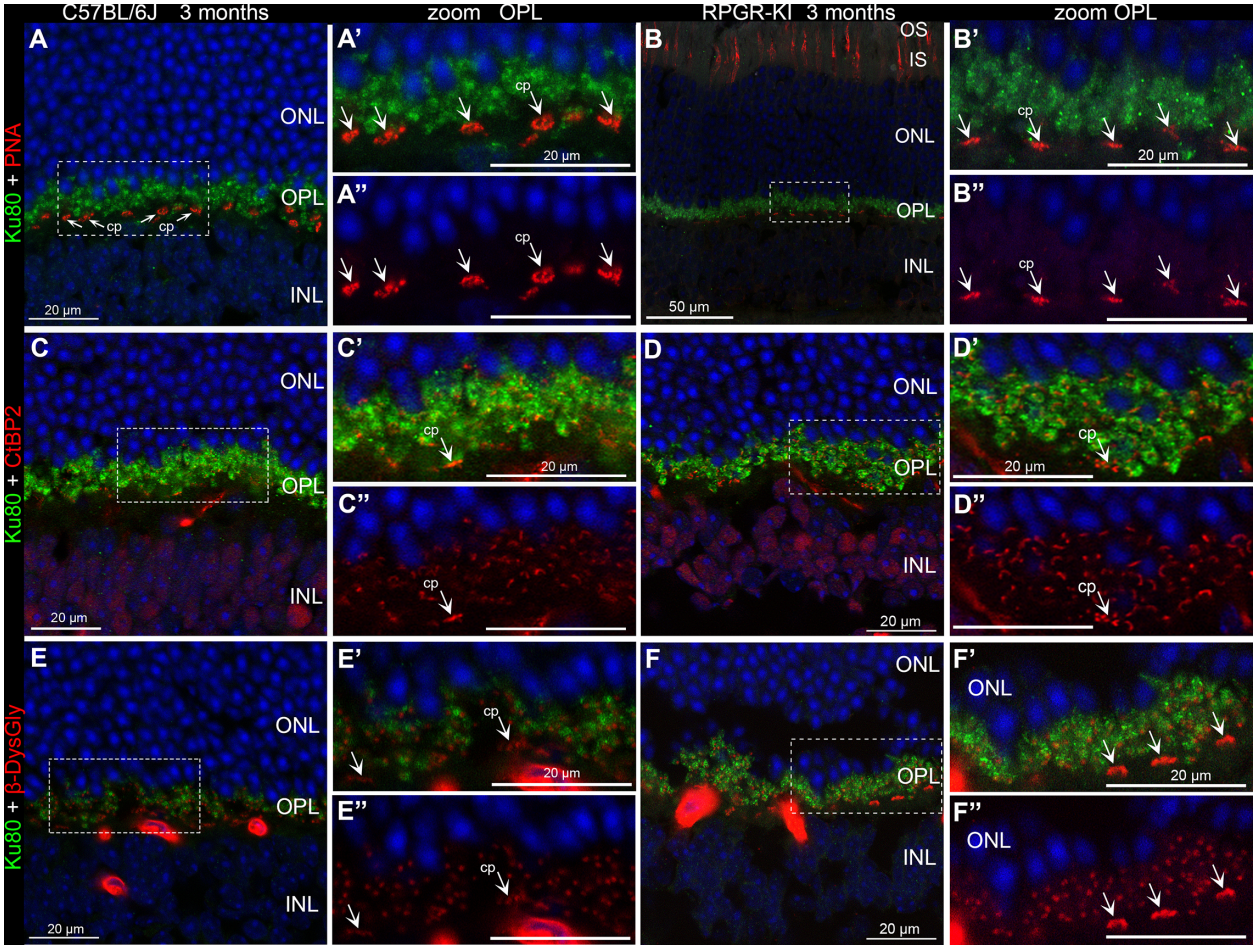

Figure 3. Localization of Ku80 in rod photoreceptor synapses in the retina of three-month-old C57BL/6J and RPGR-KI mice (B6J.SV129-^{Rpgrtm1stie}). Double and single immunolabeling are displayed in combination with DAPI staining (*blue*). (**A, B**) Double immunolabeling of Ku80 (*green*) and PNA (*red*). (**A', A″, B', B″**) Magnification of the OPL. PNA is localized in cone photoreceptor outer segments and synapses, the cone pedicles (*arrows*). Ku80 immunostaining does not co-localize with cone pedicles (**A', B'**). (**C, D**) Double immunolabeling of Ku80 (*green*) and CtBP2 (*red*). CtBP2 labels ribbon like structures in photoreceptor synapses. Numerous horseshoe-shaped rod ribbons are visible in the OPL assigning the layer of the rod spherules (**C″, D″**). CtBP2-ir ribbons in cones pedicles are lining up below and outside the Ku80 immunolabeling in the OPL (*arrow* in **C', D'**). (**E, F**) Double immunolabeling of Ku80 (*green*) and β-dystroglycan (*red*). Beta-dystroglycan is present in all photoreceptor synapses. *Arrows* indicate β-dystroglycan immunolabeling in cone pedicles (**E', E″, F', F″**). The strongly labeled red profiles are cross sectioned blood vessels (capillaries) detected by the secondary antibody directed against mouse. IS, inner segments; cp, cone pedicle. *Scale bars* are indicated in the respective pictures.

was found in the OPL because of the potassium bromate treatment.

Ku80 Is Expressed in Photoreceptors and Expression Increases Over Time During Degeneration

We performed quantitative PCR to study mRNA levels in organotypic retina culture to refine our understanding of the Ku80 expression in the retina during neurodegeneration (Fig. 7). While in whole wild-type organotypic retina culture, relative *Ku80* expression was between two- to threefold higher compared to uncultured whole retina (Fig. 7A), it was stable in whole RPGR-KI organotypic retina culture (i.e., not much different to uncultivated retina [0.5 ± 0.4 to 1.2 ± 1.23]). At days 4 and 6 Ku80-fold change was significantly different between the two mouse lines. To investigate the *Ku80* gene expression in the photoreceptor layer, we performed LCM. With this method, we compared the *Ku80* expression in the ONL at the respective cultivation stage with ONL of uncultured retina. We were able to detect relative gene expression of *Ku80* with LCM in organotypic retina culture for up to six days (Fig. 7B). Interestingly, in the ONL of wild-type retinal explant culture, we discovered a similar increase in *Ku80* gene expression as in whole retina (i.e., between two- and threefold higher compared to uncultured whole retina). Mean values increased from day 1 (1.5 ± 0.7) to day 6 (3.1 ± 1.9). Likewise, to our results for whole retina, relative Ku80 gene expression in the ONL of RPGR-KI retinal culture remained stable or even slightly decreased with time in culture compared to ONL of uncultured retina. These observations show an upregulation of *Ku80* expression in response to degenerative processes in the retina only in wild-type mice and not in our RPGE-KI mouse model. Because degenerative processes in photoreceptors induce an increased number of DSBs and are associated with apoptotic mechanisms, these observations indicate an increased readiness of the retina to DSB repair in general.

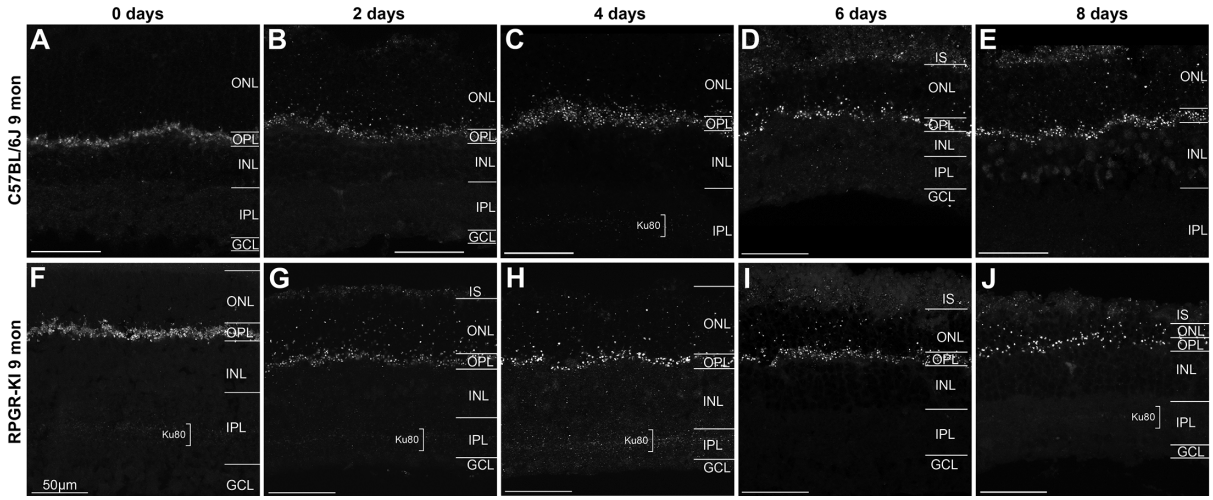

Figure 4. Release of Ku80 during retinal explant culture into the ONL. Vertical frozen sections of nine-month-old C57BL/6J mice and RPGR-KI mice (B6J.SV129-Rpgr^{tm1stie}) were evaluated. Strong Ku80 immunoreactivity is obvious in the OPL of the retina in both mouse lines (**A–J**). Ku80-ir globules were translocated into the ONL during retinal explant culture. In addition, especially in the IPL of RPGR-KI mice Ku80 immunoreactivity was visible in a week spotty manner (level marked by the *bracket*). Weak nuclear Ku80 immunoreactivity only occurred in nuclei of the INL in wild-type mice after eight days in culture (**E**). In RPGR-KI mice only very faint Ku80 immunoreactivity was detectable in INL nuclei after four days in culture (**H**). IS, inner segments; GCL, ganglion cell layer. *Scale bars*: 50 µm.

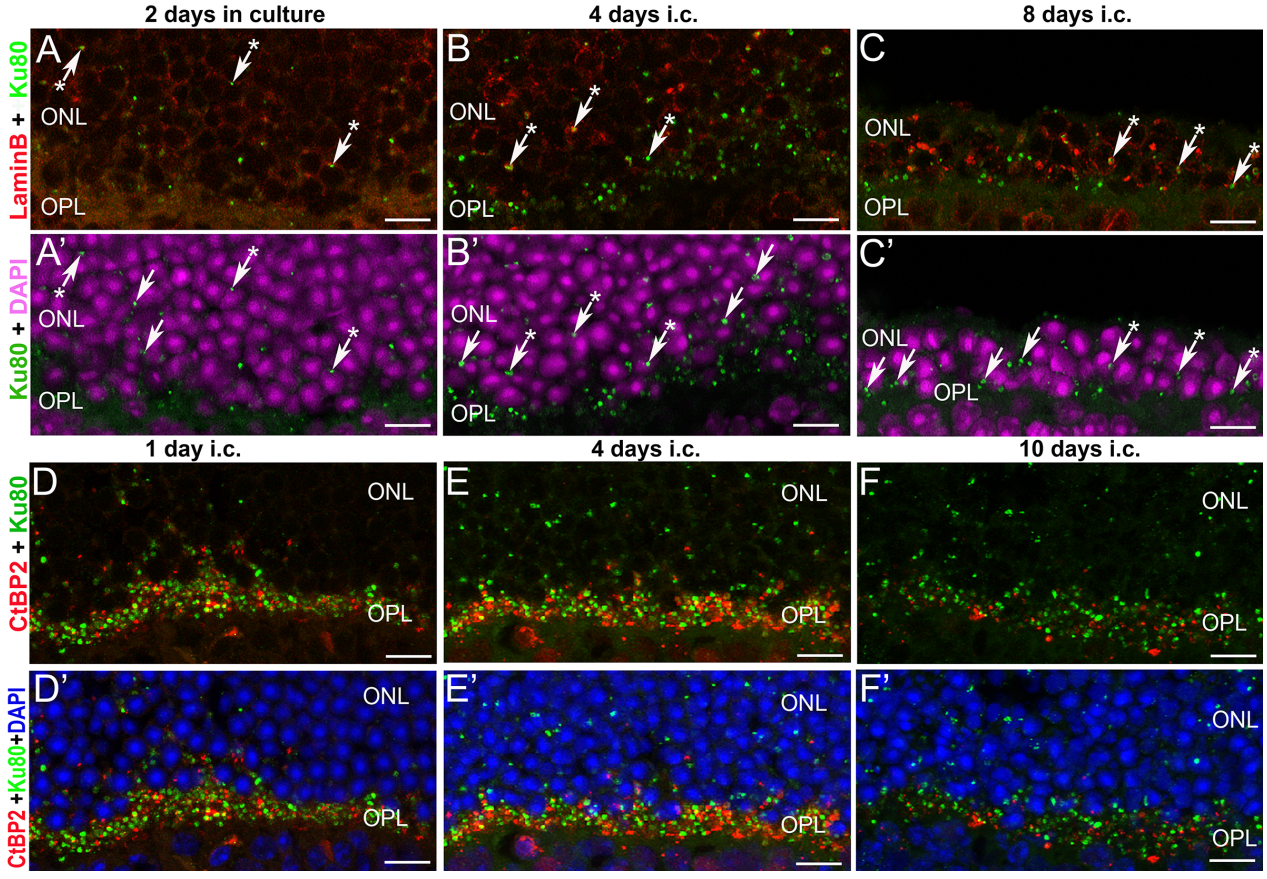

Figure 5. Release of Ku80 globules and dislocation of rod photoreceptor synapses to the ONL during retinal explant culture. Nine-month old C57BL6/J mice were evaluated after one to 10 days. (**A-C'**) Vertical frozen sections were immunolabeled with LaminB monoclonal (red) and Ku80 polyclonal antibody (*green*). LaminB antibody labels nuclear membrane of photoreceptor nuclei in the ONL (**A–C**). Counterstaining with DAPI (*magenta* or *blue*) reveals the inverse chromatin arrangement of rod photoreceptor nuclei in the ONL (**A'-C'**). *Arrows* indicate Ku80-ir globules in the periphery of the photoreceptor nuclei (euchromatin; lighter DAPI staining). Ku80-ir globules clearly located close to the LaminB-ir nuclear membrane are marked by *arrow* + *asterisk*. Frozen sections labeled with CtBP2 (*red*) and Ku80 (D-F') show dislocation of photoreceptor ribbon synapses into the ONL in addition to the translocated Ku80-ir globules from day 1 onward of retinal explant culture. At 10 days in culture very few CtBP2-ir ribbon synapses are left in the OPL and none in the ONL. All *scale bars*: 10 µm.

Investigative Ophthalmology & Visual Science

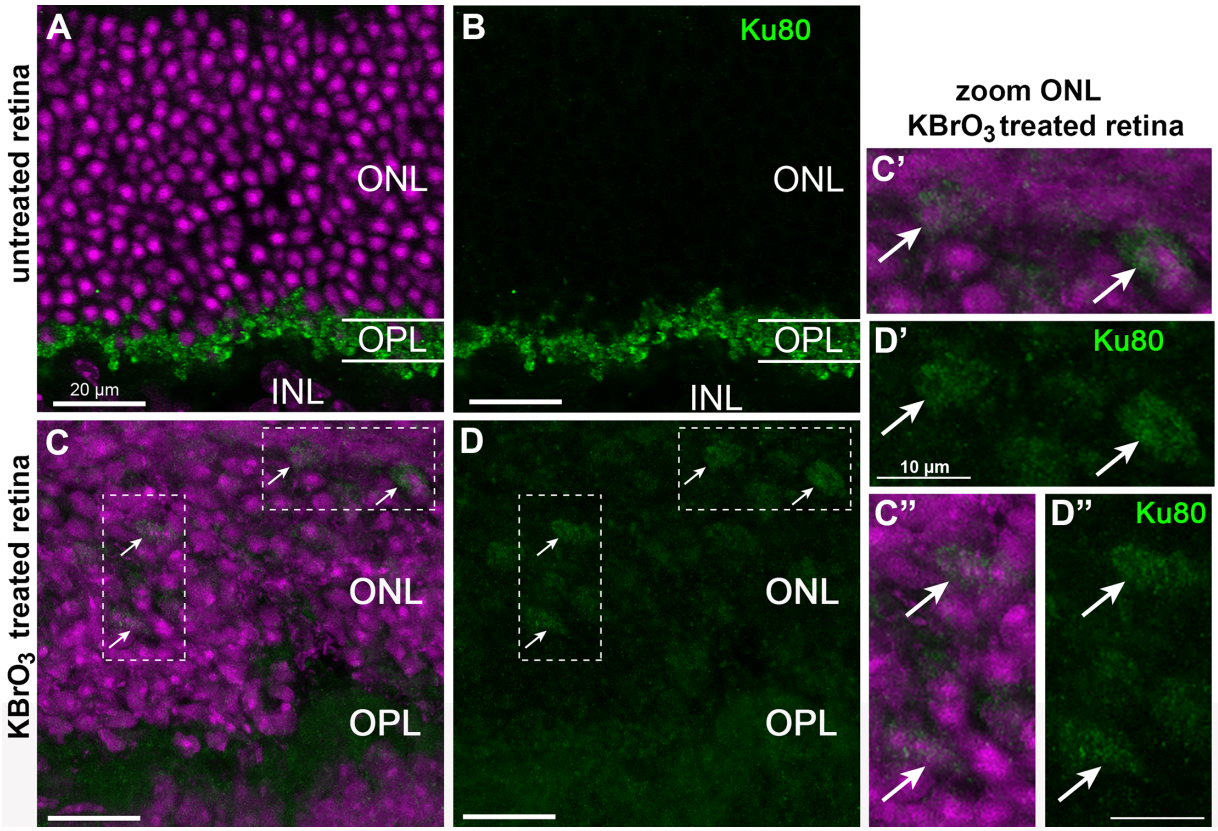

Figure 6. DNA double strand breaks induce Ku80 protein expression in photoreceptor nuclei. Vertical frozen sections of four-month-old RPGR-KI mice (B6J.SV129-^{Rpgrtm1stie}) untreated (**A, B**) and treated with 0.15 mM $KBrO_3$ for 1.5 h (**C-C″**) and immunolabeled with Ku80 antibody (*green*). DAPI counterstaining (*magenta*) reveals the nuclei of the ONL (**A, C, C', C″**). $KBrO_3$treated retina revealed Ku80 immunoreactivity in some photoreceptor nuclei, possibly cones (magnified inserts of the ONL, **C', C″, D', D″**). In untreated retina Ku80 is localized in OPL. In the ONL no Ku80 immunoreaction could be observed (**A, B**). *Scale bars* are indicated in the respective pictures.

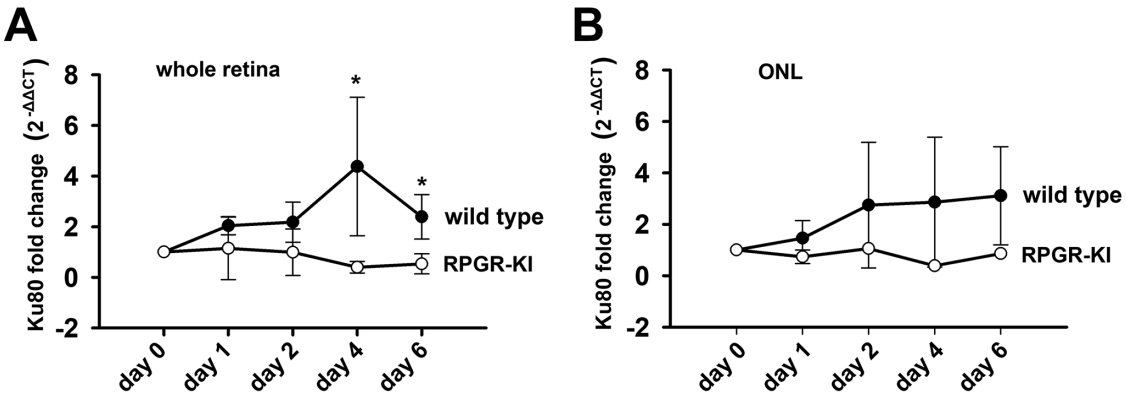

Figure 7. Relative gene expression of Ku80 in organotypic retina culture. Three-month-old C57BL/6J (wild-type) and RPGR-KI mice were analyzed after zero to six days in culture. (**A**) Ku80-fold change in organotypic retina culture of whole retina compared to uncultured (day 0) retina (n = 3 biological replicates, quantitative PCR after reverse transcription). After normalization to the reference gene Gapdh, a ratio = $2^{-\Delta\Delta Ct}$ (cultivated versus uncultured retina) >1 was considered as upregulation, whereas a ratio <1 was considered as downregulation of mRNA levels, which represent the gene expression levels. Statistical comparison of fold changes by *t*-test between mouse lines revealed significant upregulation in wild-type mice at day 4 ($P = 0.033$) and at day 6 ($P = 0.014$). (**B**) Fold change of Ku80 in ONL during organotypic retina culture using LCM to isolate the ONL. After normalization to the reference gene 18SRNA, the ratio = $2^{-\Delta\Delta Ct}$ of dissected ONL of cultured retina versus dissected ONL of day 0 retina (uncultured retina) was built. Mean values (biological replicates) were n ≤ 3. Marker gene for the ONL analysed by LCM was rhodopsin to prevent cross-contamination between individual retinal layers with the LCM method. All results are normalized to uncultured retina, that is, either whole retina (**A**) or ONL (**B**). For detailed description, see results. *Error bars* in A & B indicate SD, * $P < 0.05$ (*t*-test).

Discussion

The Ku80 protein is a key player in the DNA-DSB-repair pathway NHEJ.[14] Usually, DNA-repair proteins are mainly localized in the nucleus during interphase in various human cell lines.[15,38,39] Here, in all mouse lines investigated, we observed strong Ku80 immunoreactivity in the OPL of the retina, irrespective of age. Using antibodies against different marker proteins expressed in PR terminals, we observed specific localization of Ku80 in rod spherules. In double immunolabeling with Ku80 and β-dystroglycan, we clearly showed that Ku80 was localized in rod spherules but not in cone pedicles. PNA, which labels cone pedicles only, showed no colocalization with the Ku80 protein. These results were quite unexpected but are in line with further data on DSB repair in murine PRs. Recently, it had been shown that DNA DSB repair in murine PRs differs to other cells of the body, both in time course and repair proteins involved.[8,10,13,40,41] The different status of the DSB repair proteins in rod PRs was corroborated by the fact that p53 binding protein 1 (53bp1), another important repair protein in the pathway of repair proceeding NHEJ, was not detectable unequivocally in rod PRs.[13] The 53bp1 stained foci only rarely occurred in rod PRs and colocalization of 53bp1 and γH2AX-positive foci was a very rare event compared to DNA repair foci labeled with the two markers in dividing cells.[40,41]

In the present study, detection of Ku80-ir globules close to the Lamin B-ir nuclear membrane of rod PR nuclei during retinal explant culture argue for translocation of Ku80 globules from the rod spherules into the ONL during neurodegeneration. This can well be seen as a response of the cell to increasing damage of the DNA during early phases of cell stress and increased numbers of DSBs. In adult mouse retina, Lamin B protein is highly expressed in the nuclear membrane of ganglion cells and moderately in the nuclei of the INL. Rod PRs show only weak Lamin B immunostaining.[13] The hypothesis of Ku80 release from the rod PR terminals to the nuclear area during retinal explant culture was corroborated by Ku80-ir globules localized in the lightly stained euchromatin area located in the periphery of the murine rod PR nuclei, where active genes are transcribed and telomers can be found.[9] In addition, we showed by co-staining with CtBP2 that the relocalization of the globules into the nuclear layer was associated with stress during retinal organ culture and degeneration of PRs, starting with retraction of the rod terminals, a common scheme observed in degenerative retinae.[42] However, even at day 1, where most CtBP2-ir ribbons were obvious in the ONL compared to later stages of retinal explant culture, far more Ku80-ir globules were detectable.

Two decades ago, unexpected localization of Ku80 protein in the cytoplasm was detected by immunohistochemistry in both immature and mature cerebral cortex.[43] In mature brains, fewer Ku80-ir neurons were found. Even though Ku is known as a nuclear protein, its cytoplasmic localization has been also shown in lymphocytes by Western blotting of cytoplasmic, nuclear, and whole cell extracts.[44] The translocation of Ku between cytoplasm and nuclei was observed in the progression of cell cycle and in CD-40 mediated events, suggesting some physiological significance of the subcellular distribution.[44] Concerning the Ku80 translocation, it is known that it has a nuclear localization signal that is conserved in human, canine, and mouse Ku80.[45] It is hypothesized that the nuclear localization signal is also used to export Ku80 from the nucleus. Therefore we can only speculate about the translocation and assume that in murine photoreceptors the Ku80 protein is translocated into rod spherules for storage and translocated toward the nucleus on DNA DSBs.

Direct Ku80 protein detection by immunohistochemistry and Western blot and upregulated relative *Ku80* expression in whole retina preparations, as well as in individual retinal layers (ONL), demonstrated the presence of this important protein in murine retinal neurons. Analysis of relative *Ku80* expression by qPCR revealed a constant slight upregulation within the whole retina during retinal explant culture by up to twofold compared to uncultured retinae. With LCM, we were able to compare the *Ku80* expression in the ONL during retinal explant culture with ONL of uncultured retina samples and found a similar increase in expression as in whole retina for both wild-type and RPGR-KI mice. Although preliminary, this further corroborates the notion that Ku80 protein is expressed in photoreceptors and is released and upregulated during degeneration. Colocalization with Ku70 as its natural partner molecule to form the Ku complex was not possible because the Ku70 antibody, at least in our hand, did not work in the murine retina.

In general, the results of our study are difficult to compare with studies using irradiation to create DNA DSBs because the cells' own DNA repair mechanisms may differ depending on the damage-causing agent. Ionizing radiation causes exogenous DNA damage,[46] whereas during retinal explant culture endogenous DNA damage occurs.[5] The fact that Ku80 is an important component of DNA DSB repair, and that Ku80 deficiency leads to extreme sensitivity to ionizing radiation is well known from studies on cancer tissue.[47,48] In diverse malignant tumors, such as in the bladder or the breast, an upregulation of Ku80 occurs, which implies that Ku80 is a tumor-promoting factor.[49,50] Consequently, the defects in tumor cells include defects in the repair of DSBs.

In conclusion, we could show unequivocally the presence of the DNA DSB repair protein Ku80 in the murine retina and revealed its unexpected location in the terminals of rod photoreceptor cells. This indicates once again that tissue-specific modifications to the canonical DNA repair mechanisms in murine rod photoreceptors, which account for 97% of all photoreceptors in the mouse retina,[51] and warrant further investigation. The knowledge about the DSB repair mechanisms in all retinal neurons is the prerequisite for future genome editing strategies for inherited retinal disease.

Acknowledgments

The supply of eyes of one-month-old mice of the degenerating mouse line rd10 and their respective wild-type C57BL/6J by Paquet-Durand of the Institute for Ophthalmic Research, University of Tübingen, is gratefully acknowledged. The use of the LCM facility in the Medical Clinic II, Excellence Cluster Cardio-Pulmonary System (ECCPS) by Norbert Weissmann, Justus-Liebig-University Giessen, is gratefully acknowledged.

Supported by the German Research Society (DFG) priority program SPP2127 – gene and cell based therapies to counteract neuroretinal degeneration.

Disclosure: **B. Müller,** None; **F. Serafin,** None; **L.L. Laucke,** None; **W. Rheinhard,** None; **T. Wimmer,** None; **K. Stieger,** None

References

1. Daiger S. RetNet - Retinal Information Network, https://sph.uth.edu/retnet/. Accessed June 9, 2022.
2. Verbakel SK, van Huet RAC, Boon CJF, et al. Non-syndromic retinitis pigmentosa. *Prog Retin Eye Res*. 2018;66:157–186.
3. Sengillo JD, Justus S, Cabral T, Tsang SH. Correction of monogenic and common retinal disorders with gene therapy. *Genes (Basel)*. 2017;8(2):53.
4. Osborn MJ, Belanto JJ, Tolar J, Voytas DF. Gene editing and its application for hematological diseases. *Int J Hematol*. 2016;104:18–28.
5. Yanik M, Müller B, Song F, et al. In vivo genome editing as a potential treatment strategy for inherited retinal dystrophies. *Prog Retin Eye Res*. 2017;56:1–18.
6. Deng SK, Gibb B, De Almeida MJ, Greene EC, Symington LS. RPA antagonizes microhomology-mediated repair of DNA double-strand breaks. *Nat Struct Mol Biol*. 2014;21:405–412.
7. Sakuma T, Nakade S, Sakane Y, Suzuki K-IT, Yamamoto T. MMEJ-assisted gene knock-in using TALENs and CRISPR-Cas9 with the PITCh systems. *Nat Protoc*. 2016;11:118–133.
8. Frohns A, Frohns F, Naumann SC, Layer PG, Löbrich M. Inefficient double-strand break repair in murine rod photoreceptors with inverted heterochromatin organization. *Curr Biol*. 2014;24:1080–1090.
9. Solovei I, Kreysing M, Lanctôt C, et al. Nuclear architecture of rod photoreceptor cells adapts to vision in mammalian evolution. *Cell*. 2009;137:356–368.
10. Frohns F, Frohns A, Kramer J, et al. Differences in the response to DNA double-strand breaks between rod photoreceptors of rodents, pigs, and humans. *Cells*. 2020;9(4):947.
11. Maruyama T, Dougan SK, Truttmann M, Bilate AM, Ingram JR, Ploegh HL. Inhibition of non-homologous end joining increases the efficiency of CRISPR/Cas9-mediated precise genome editing. *Nature*. 2015;33(5):538–542.
12. Chu VT, Weber T, Wefers B, et al. Increasing the efficiency of homology-directed repair for CRISPR-Cas9-induced precise gene editing in mamm. *Nat Biotechnol*. 2015;33:543–548.
13. Müller B, Ellinwood NM, Lorenz B, Stieger K. Detection of DNA double strand breaks by γH2AX does not result in 53bp1 recruitment in mouse retinal tissues. *Front Neurosci*. 2018;12:286.
14. Mahaney BL, Meek K, Lees-Miller SP. Repair of ionizing radiation-induced DNA double-strand breaks by non-homologous end-joining. *Biochem J*. 2009;417:639–650.
15. Koike M. Dimerization, Translocation and Localization of Ku70 and Ku80 Proteins. *J RADIAT RES*. 2002;43:223–236.
16. Strande N, Roberts SA, Oh S, Hendrickson EA, Ramsden DA. Specificity of the dRP/AP lyase of Ku promotes nonhomologous end joining (NHEJ) fidelity at damaged ends. *J Biol Chem*. 2012;287:13686–13693.
17. Roberts SA, Strande N, Burkhalter MD, et al. Ku is a 5'-dRP/AP lyase that excises nucleotide damage near broken ends. *Nature*. 2010;464(7292):1214–1217.
18. Tuteja R, Tuteja N. Ku autoantigen: a multifunctional DNA-binding protein. *Crit Rev Biochem Mol Biol*. 2000;35:1–33.
19. Xiao Y, Wang J, Qin Y, et al. Ku80 cooperates with CBP to promote COX-2 expression and tumor growth. *Oncotarget*. 2015;6:8046–8061.
20. Indiviglio SM, Bertuch AA. Ku's essential role in keeping telomeres intact. *Proc Natl Acad Sci USA*. 2009;106:12217–12218.
21. Koike M. Dimerization, Translocation and Localization of Ku70 and Ku80 proteins. *J Radiat Res*. 2002;43:223–236.
22. Song JY, Lim JW, Kim H, Morio T, Kim KH. Oxidative stress induces nuclear loss of DNA repair proteins Ku70 and Ku80 and apoptosis in pancreatic acinar AR42J cells. *J Biol Chem*. 2003;278:36676–36687.
23. Gu Y, Seidl KJ, Rathbun GA, et al. Growth retardation and leaky SCID phenotype of Ku70-deficient mice. *Immunity*. 1997;7:653–665.
24. Nussenzweig A, Chen C, da Costa, Soares V, et al. Requirement for Ku80 in growth and immunoglobulin V(D)J recombination. *Nature*. 1996;382(6591):551–555.
25. Schlegel J, Hoffmann J, Röll D, et al. Toward genome editing in X-linked RP—development of a mouse model with specific treatment relevant features. *Transl Res*. 2019;203:57–72.
26. Chang B, Hawes NL, Hurd RE, Davisson MT, Nusinowitz S, Heckenlively JR. Retinal degeneration mutants in the mouse. *Vision Res*. 2002;42:517–525.
27. Müller B, Wagner F, Lorenz B, Stieger K. Organotypic cultures of adult mouse retina: morphologic changes and gene expression. *Invest Ophthalmol Vis Sci*. 2017;58:1930–1940.
28. Eberhart A, Kimura H, Leonhardt H, Joffe B, Solovei I. Reliable detection of epigenetic histone marks and nuclear proteins in tissue cryosections. *Chromosom Res*. 2012;20:849–858.
29. Livak KJ, Schmittgen TD. Analysis of relative gene expression data using real-time quantitative PCR and the 2-ΔΔCT method. *Methods*. 2001;25:402–408.
30. Campbell KP, Kahl SD. Association of dystrophin and an integral membrane glycoprotein. *Nature*. 1989;338(6212):259–262.
31. Ervasti JM, Campbell KP. Membrane organization of the dystrophin-glycoprotein complex. *Cell*. 1991;66:1121–1131.
32. Drenckhahn D, Holbach M, Ness W, Schmitz F, Anderson L V. Dystrophin and the dystrophin-associated glycoprotein, beta-dystroglycan, co-localize in photoreceptor synaptic complexes of the human retina. *Neuroscience*. 1996;73:605–612.
33. Blank M, Koulen P, Blake DJ, Kröger S. Dystrophin and beta-dystroglycan in photoreceptor terminals from normal and mdx 3Cv mouse retinae . *Eur J Neurosci*. 1999;11:2121–2133.
34. Schmitz F, Drenckhahn D. Dystrophin in the retina. *Prog Neurobiol*. 1997;53:547–560.
35. Koulen P, Blank M, Kröger S. Differential distribution of beta-dystroglycan in rabbit and rat retina. *J Neurosci Res*. 1998;51:735–747.
36. Solovei I, Wang AS, Thanisch K, et al. LBR and lamin A/C sequentially tether peripheral heterochromatin and inversely regulate differentiation. *Cell*. 2013;152:584–598.
37. Bao L, Yao XS, Yau CC, et al. Protective effects of bilberry (Vaccinium myrtillus L.) extract on restraint stress-induced liver damage in mice. *J Agric Food Chem*. 2008;56:7803–7807.
38. Koike M, Ikuta T, Miyasaka T, Shiomi T. Ku80 can translocate to the nucleus independent of the translocation of Ku70 using its own nuclear localization signal. *Oncogene*. 1999;18:7495–7505.
39. Koike M, Awaji T, Kataoka M, et al. Differential subcellular localization of DNA-dependent protein kinase components Ku and DNA-PKcs during mitosis. *J Cell Sci*. 1999;112(Pt 2):4031–4039.
40. Kim JS, Krasieva TB, Kurumizaka H, Chen DJ, Taylor AMR, Yokomori K. Independent and sequential recruitment of NHEJ and HR factors to DNA damage sites in mammalian cells. *J Cell Biol*. 2005;170:341–347.

41. Mari P-O, Florea BI, Persengiev SP, et al. Dynamic assembly of end-joining complexes requires interaction between Ku70/80 and XRCC4. *Proc Natl Acad Sci USA*. 2006;103:18597–18602.
42. Cuenca N, Pinilla I, Sauvé Y, Lund R. Early changes in synaptic connectivity following progressive photoreceptor degeneration in RCS rats. *Eur J Neurosci*. 2005;22:1057–1072.
43. Oka A, Takashima S, Abe M, Araki R, Takeshita K. Expression of DNA-dependent protein kinase catalytic subunit and Ku80 in developing human brains: implication of DNA-repair in neurogenesis. *Neurosci Lett*. 2000;292:167–170.
44. Morio T, Hanissian SH, Bacharier LB, et al. Ku in the cytoplasm associates with CD40 in human B cells and translocates into the nucleus following incubation with IL-4 and anti-CD40 mAb. *Immunity*. 1999;11:339–348.
45. Koike M, Yutoku Y, Koike A. Cloning of canine Ku80 and its localization and accumulation at DNA damage sites. *FEBS Open Bio*. 2017;7:1854–1863.
46. Chatterjee N, Walker GC. Mechanisms of DNA damage, repair, and mutagenesis. *Environ Mol Mutagen*. 2017;58:235–263.
47. Nimura Y, Kawata T, Uzawa K, et al. Silencing Ku80 using small interfering RNA enhanced radiation sensitivity in vitro and in vivo. *Int J Oncol*. 2007;30:1477–1484.
48. Li F, Sun Q, Liu K, et al. The deubiquitinase OTUD5 regulates Ku80 stability and non-homologous end joining. *Cell Mol Life Sci*. 2019;76:3861–3873.
49. Kruer TL, Cummins TD, Powell DW, Wittliff JL. Characterization of estrogen response element binding proteins as biomarkers of breast cancer behavior. *Clin Biochem*. 2013;46(16-17):1739–1746.
50. Groselj B, Kerr M, Kiltie AE. Radiosensitisation of bladder cancer cells by panobinostat is modulated by Ku80 expression. *Radiother Oncol*. 2013;108:429–433.
51. Jeon CJ, Strettoi E, Masland RH. The major cell populations of the mouse retina. *J Neurosci*. 1998;18:8936–8946.

Investigative Ophthalmology & Visual Science